BIOCHEMICAL PHARMACOLOGY 76 (2008) 531–542

available at www.sciencedirect.com

ScienceDirect

journal homepage: www.elsevier.com/locate/biochempharm

Identification of the functional vitamin D response elements in the human *MDR1* gene

Mayumi Saeki, Kouichi Kurose, Masahiro Tohkin, Ryuichi Hasegawa*

Division of Medicinal Safety Science, National Institute of Health Sciences, 1-18-1 Kamiyoga, Setagaya-ku, Tokyo 158-8501, Japan

ARTICLE INFO

Article history:
Received 25 March 2008
Accepted 22 May 2008

Keywords:
Multidrug resistance 1
P-glycoprotein (P-gp)
Vitamin D receptor (VDR)
1α,25-Dihydroxyvitamin D_3
Vitamin D response element (VDRE)

ABSTRACT

P-glycoprotein, encoded by the multidrug resistance 1 (*MDR1*) gene, is an efflux transporter and plays an important role in pharmacokinetics. The expression of *MDR1* is induced by a variety of compounds, of which 1α,25-dihydroxyvitamin D_3 is known to be an effective inducer. However, it remains unclear how 1α,25-dihydroxyvitamin D_3 regulates the expression of *MDR1*. In this study, we demonstrated that the vitamin D receptor (VDR) induces *MDR1* expression in a 1α,25-dihydroxyvitamin D_3-dependent manner. Luciferase assays revealed that the region between −7.9 and −7.8 kbp upstream from the transcription start site of the *MDR1* is responsible for the induction by 1α,25-dihydroxyvitamin D_3. Electrophoretic mobility shift assays revealed that several binding sites for the VDR/retinoid X receptor α (RXRα) heterodimer are located between the −7880 and −7810 bp region, to which the three molecules of VDR/RXRα are able to simultaneously bind with different affinities. Luciferase assays using mutated constructs revealed that the VDR-binding sites of DR3, DR4(I), MdC3, and DR4(III) contribute to the induction, indicating that these binding sites act as vitamin D response elements (VDREs). The contribution of each VDRE to the inducibility was different for each response element. An additive effect of the individual VDREs on induced luciferase activity by 1α,25-dihydroxyvitamin D_3 was also observed. These results indicate that the induction of *MDR1* by 1α,25-dihydroxyvitamin D_3 is mediated by VDR/RXRα binding to several VDREs located between −7880 and −7810 bp, in which every VDRE additively contributes to the 1α,25-dihydroxyvitamin D_3 response.

1. Introduction

P-glycoprotein (P-gp), which is encoded by the multidrug resistance 1 (*MDR1*) gene, transports a wide range of compounds, such as drugs and xenobiotics, from intracellular to extracellular compartments [1]. P-gp is expressed on the apical surface of epithelial cells of tissues including intestine, kidney, liver, and brain, and plays an important role in drug absorption, renal secretion, biliary excretion, and brain distribution [1]. CYP3A4 is the most abundantly expressed human cytochrome P450 contributing to drug metabolism, and P-gp and CYP3A4 share many substrates, inhibitors, inducers, and tissue distribution patterns [2]. Therefore, it has been hypothesized that the expressions of MDR1 and CYP3A4 have similar regulatory mechanisms. In fact, both genes are directly regulated by nuclear receptors, pregnane X receptor (PXR) and constitutive androstane receptor (CAR) [3–6].

Previous reports revealed that 1α,25-dihydroxyvitamin D_3 (1,25-$(OH)_2D_3$), the most active metabolite of vitamin D_3, regulates the expression of MDR1 mRNA and P-gp protein. The treatment of LS180 cells, a human colon carcinoma cell line, with 1,25-$(OH)_2D_3$ led to a significant increase in MDR1 mRNA and P-gp protein levels [7–9]. In human airway epithelium-derived Calu-3 cells, treatment with 1,25-$(OH)_2D_3$ caused

* *Corresponding author*. Tel.: +81 3 3700 9789; fax: +81 3 3700 9788.
E-mail address: kurose@nihs.go.jp (K. Kurose).
0006-2952/$ – see front matter
doi:10.1016/j.bcp.2008.05.030

elevated P-gp expression [10]. Furthermore, Olaizola et al. reported that the uptake of [^{99m}Tc]-sestamibi (which is known to be a substrate of P-gp and is excreted by P-gp [11,12]) by the parathyroid glands of uremic patients was suppressed by pulse administration of 1,25-$(OH)_2D_3$ for 2 weeks, suggesting that P-gp induction by 1,25-$(OH)_2D_3$ leads to increased [^{99m}Tc]-sestamibi efflux [13].

The biological activity of 1,25-$(OH)_2D_3$ is mainly mediated via the vitamin D receptor (VDR), a member of the nuclear receptor superfamily. VDR forms a heterodimer with retinoid X receptor (RXR) and binds to the vitamin D response element (VDRE) in the regulatory region of genes. The VDRE by which the gene is regulated positively is generally composed of a direct repeat (DR) of the consensus hexamer (half-site) sequence of 5′-RGKTCA-3′ (R = A or G, and K = G or T) spaced by three or four nucleotides (DR3 or DR4), or an everted repeat spaced by 6, 7, 8, or 9 nucleotides (ER6, ER7, ER8, or ER9) [14–17]. However, negative response elements for 1,25-$(OH)_2D_3$ have been identified in several genes down-regulated by 1,25-$(OH)_2D_3$, such as human pituitary transcription factor-1 gene, in which an imperfect DR2 motif acts as a negative VDRE [18].

Previously, Geick et al. reported that the induction of *MDR1* by rifampin is mediated by PXR which binds to a DR4 located between −7.9 and −7.8 kbp upstream from the transcription start site [3]. Burk et al. reported that CAR also induces *MDR1* expression by binding to several DR4s located in the same region [4]. Recently, we reported that thyroid hormone receptor (TR) regulates the expression of *MDR1* by binding to several DRs located in the same region [19]. It was reported that 1,25-$(OH)_2D_3$ also regulates CYP3A4 induction through the binding of VDR/RXRα to some PXR response elements [14]. These results suggest that VDR also binds to several DR motifs in the same region of the *MDR1* gene and regulates the expression of *MDR1*. However, this theory requires substantiation.

There is variation amongst individuals in intestinal *MDR1* expression [20]. Since 1,25-$(OH)_2D_3$ induces the expression of *MDR1*, the 1,25-$(OH)_2D_3$-mediated induction process might be involved in this inter-individual variation. Furthermore, vitamin D is widely prescribed and influences the induction of P-gp, which potentially affects pharmacokinetics. Therefore, the role of vitamin D in the mechanism of *MDR1* expression is worthy of investigation. In this study, we investigated that how 1,25-$(OH)_2D_3$ regulates the expression of *MDR1* using the intestinal epithelial cell line Caco-2. We demonstrate that the induction of *MDR1* by 1,25-$(OH)_2D_3$ is mediated by VDR/RXRα binding to several VDREs located between −7880 and −7810 bp upstream of the *MDR1* gene, in which every VDRE additively contributes to the 1,25-$(OH)_2D_3$ response.

2. Materials and methods

2.1. Plasmid constructs

Human VDR cDNA was amplified from human kidney Marathon-Ready cDNA (Clontech Laboratories Inc., Palo Alto, CA, USA) with the primers 5′-ATGGAGGCAATGGCGGC-3′ and 5′-TCAGGAGATCTCATTGCCAAACAC-3′ using a TaKaRa LA Taq (Takara Bio Inc., Shiga, Japan). The resulting DNA fragment was subcloned into the pEF6/V5-His-TOPO vector (Invitrogen, Carlsbad, CA, USA) and this expression plasmid (pEF6/V5-hVDR) was used for the transfection. The sequences were verified by DNA sequencing. The pEF6/V5-hVDR plasmid was digested with KpnI (Toyobo, Osaka, Japan) and NotI (Takara Bio Inc.), and the resulting fragment was ligated into the pCMVTNT expression plasmid (Promega, Madison, WI, USA), which was digested with KpnI and NotI. This plasmid (pCMVTNT-hVDR) was used for the in vitro synthesis. The expression plasmid encoding human RXRα cDNA (pcDNA3.1-hRXRα) was a generous gift from Dr. Shuichi Koizumi (Yamanashi University, Japan). Luciferase reporter gene plasmids containing various lengths of the human *MDR1* 5′-flanking sequence were previously constructed in our laboratory [19]. Mutations in several half-sites were introduced into the pMD*824Δ90L reporter plasmid using a QuikChange Multi Site-Directed Mutagenesis kit (Stratagene, La Jolla, CA, USA) according to the manufacturer's instructions, with the previously described oligonucleotides and the following oligonucleotides, used alone or in combination: M28, 5′-GCTCCTGGGAGAGAGAACATTTGAGATTAAACAAG-3′; M31, 5′-GAACTAACTTGACCTTTTTCCTGGGAGAGAGTTC-3′; M33, 5′-AAATGAACTCAATCCCAGGAGCAAG-3′. For the M28, M29, M30, and M36 mutants shown in Fig. 4A, mutations were introduced into the M1, M3, M12, and M23 constructs using the M28 primer. For the M38 mutant shown in Fig. 4A, a deletion mutant was obtained by chance when we attempted to create the M30 mutant. All mutations were verified by DNA sequencing.

2.2. Cell culture

Caco-2 cells, a human colon adenocarcinoma cell line, were obtained from American Type Culture Collection (Manassas, VA, USA). Caco-2 cells were cultured in low glucose Dulbecco's modified Eagle's medium (DMEM, Sigma–Aldrich, St. Louis, MO, USA) supplemented with 10% heat-inactivated fetal bovine serum (FBS), 100 U/mL penicillin G/100 μg/mL streptomycin (Gibco-Invitrogen, Carlsbad, CA, USA), and 1× MEM non-essential amino acids solution (Gibco-Invitrogen) at 37 °C under 5% CO_2–95% air.

2.3. Transfection and luciferase reporter gene assays

Caco-2 cells were seeded into 96-well plates (1.6×10^4 cells/well), grown overnight, and transiently transfected using HilyMax (at a ratio of DNA to HilyMax of 1:5; Dojindo Laboratories, Kumamoto, Japan) according to the manufacturer's instructions with 10 ng/well of VDR expression plasmid (pEF6/V5-hVDR), 100 ng/well of the indicated luciferase reporter plasmid, and 10 ng/well of the *Renilla* luciferase reporter plasmid, pGL4.74 [hRluc/TK] (Promega) to normalize the transfection efficiency. After 24 h, the medium was replaced by phenol red-free DMEM (Gibco-Invitrogen) supplemented with 10% dextran-coated charcoal-stripped FBS (Hyclone Laboratories, Logan, UT, USA) containing 25 nM 1,25-$(OH)_2D_3$ (Sigma–Aldrich) or dimethyl sulfoxide (DMSO) for 3.5 h. Firefly and *Renilla* luciferase activities were measured using a Dual-Glo Luciferase Assay System (Promega) according to the manufacturer's instructions and a luminometer (Wallac 1420 ARVO sx Multilabel counter, PerkinElmer Life Sciences, Boston, MA, USA). Firefly luciferase activity was normalized to

Renilla luciferase activity, and the inducibility was calculated as the ratio of luciferase activity of 1,25-$(OH)_2D_3$-treated cells to that of control (DMSO-treated) cells. The results represent the mean ± S.D. of four independent experiments, and in each of these experiments the control and 1,25-$(OH)_2D_3$ treatments were performed at least in triplicate.

2.4. Electrophoretic mobility shift assays (EMSAs)

TNT T7 and SP6 Quick Coupled Transcription/Translation Systems (Promega) were used for in vitro synthesis of human RXRα protein from pcDNA3.1-hRXRα and human VDR protein from pCMVTNT-hVDR, respectively, according to the manufacturer's instructions. The plus strand sequences of probes and competitors used in EMSA are shown in Figs. 2A and 3A. The nonspecific competitor was double-stranded oligonucleotide located in the −218 to −117 region of the human PXR promoter [21]. The oligonucleotides, except for longer probes described below, were purchased from Sigma Genosys (Hokkaido, Japan) and equal amounts of complimentary strands were annealed. The longer probes, except for the 7882 probe shown in Fig. 3A, were prepared by polymerase chain reaction (PCR) amplification as described previously [19]. The reaction mixture used to obtain the results shown in Fig. 2B–D was prepared as follows: 2.5 μL aliquots of the in vitro translated proteins (VDR or RXRα alone, or mixed at a ratio of 1:1) or unprogrammed reticulocyte lysate were incubated for 20 min at room temperature with 1 μL of 5× binding buffer [15 mM $MgCl_2$, 0.5 mM EDTA, 2.5 mM dithiothreitol (DTT), 50% glycerol and 100 mM HEPES, pH 7.75], 0.5 μL of 1 mg/mL poly(dI–dC) (GE Healthcare UK Ltd., Buckinghamshire, UK), and 0.5 μL of 0.33 μM 5′-fluorescein isothiocyanate (FITC)-labeled double-stranded oligonucleotide probe. For competition assays, 0.5 μL of unlabeled oligonucleotide was simultaneously added to the reaction mixture with the probe. For the assays used to obtain the results shown in Fig. 3, 2–8 μL (Fig. 3B) or 8 μL (Fig. 3C) of the in vitro translated VDR and RXRα mixed at a ratio of 1:1 were used, if necessary, the volume of which was adjusted to 8 μL with unprogrammed reticulocyte lysate. The 8-μL aliquots of the proteins were incubated for 20 min at room temperature with 1 μL of 10× binding buffer (30 mM $MgCl_2$, 1 mM EDTA, 5 mM DTT, 50% glycerol and 200 mM HEPES, pH 7.75), 0.5 μL of 1 mg/mL poly(dI–dC), and 0.5 μL of the PCR-based probe or 0.33 μM 5′-FITC-labeled 7882 probe in the presence or absence of 250 nM 1,25-$(OH)_2D_3$. The 1.5-μL aliquots of the protein–DNA complexes were resolved by electrophoresis on 2.8 or 6% non-denaturing Long Ranger gels (Lonza, Basel, Switzerland) run in 0.5× TBE (44.5 mM Tris, 44.5 mM boric acid, and 1.25 mM EDTA) at 500 V constant voltage, and visualized and quantified on a slab gel DNA sequencer DSQ-2000L (Shimadzu Co., Kyoto, Japan).

3. Results

3.1. Identification of the 1,25-$(OH)_2D_3$-responsive region in the MDR1 gene

To investigate the mechanism of *MDR1* gene expression induced by 1,25-$(OH)_2D_3$, we performed a luciferase reporter gene assay using an intestinal epithelial cell line, Caco-2, which expresses VDR at relatively lower level [9]. The cells were transfected with a reporter plasmid containing the 5′-upstream region from −10082 to +117 bp of *MDR1* (pMD10082L) in the presence or absence of an expression plasmid encoding VDR. Following the treatment with either vehicle (DMSO) or 1,25-$(OH)_2D_3$, luciferase assays were performed. In the absence of VDR expression plasmid, 1,25-$(OH)_2D_3$ had little affect on the transcriptional activity. By contrast, in the presence of VDR expression plasmid, more than an eightfold activation was induced by 1,25-$(OH)_2D_3$ (Fig. 1A). These results indicate that the 1,25-$(OH)_2D_3$-responsive region is located within 10 kbp of the 5′-flanking region of *MDR1*, and that VDR mediates *MDR1* induction by 1,25-$(OH)_2D_3$.

Next, to identify the response elements implicated in the transcriptional regulation of *MDR1* by 1,25-$(OH)_2D_3$, we performed luciferase assays using several deletion mutants of pMD10082L. As shown in Fig. 1A, the 824 bp deletion from −7970 to −7145 bp resulted in the complete loss of inducibility. The lost inducibility was recovered by reinsertion of the deleted region of 824 bp (Fig. 1A, bottom line, pMD*824L). These results indicate that the 824 bp region is essential for the induction of *MDR1* by 1,25-$(OH)_2D_3$.

To further define the minimal region for the VDR response, deletion analysis was performed based on pMD*824L, which contains the 824 bp region (Fig. 1B). The 90 bp deletion from the 5′-end did not affect inducibility, whereas the 153 bp deletion from the 5′-end resulted in the complete loss of inducibility. These data suggest that the essential region for the VDR-mediated induction is located between −7880 and −7817 bp.

3.2. VDR binds to the putative VDRE as a heterodimer with RXRα

We scanned the 1,25-$(OH)_2D_3$ response region between −7880 and −7810 bp using the JASPAR FAM database (http://jaspar.genereg.net/). Several putative half-sites, a pair of which composes a DR or ER, were found (Hs1–8, Fig. 2A). Generally, some DRs or ERs, including DR3 and DR4 (which lie in this region, as shown in Fig. 2A) act as VDRE.

The region including the putative VDRE was divided into three segments, designated upstream cluster (UpC), middle cluster (MdC), and downstream cluster (DwC); we have reported this convenient classification previously [19]. Each cluster has several putative half-sites. To determine whether VDR and RXRα could bind directly to these segments, EMSA was performed using in vitro translated VDR and RXRα. The probes and competitors used for the EMSA are summarized in Fig. 2A. The DNA–protein complexes were formed in the presence of both VDR and RXRα, although the complexes were not formed in the absence of either protein, indicating that the protein complex VDR/RXRα binds to each segment (Fig. 2B–D). The DNA–protein complexes were competed out by the self-competitors but were not competed out by the nonspecific competitor (Fig. 2B–D). The relative affinities of VDR/RXRα to UpC, MdC, and DwC were further assessed by competition experiments. As shown in Fig. 2B, the complexes of UpC with VDR/RXRα were competed out by competitors UpC, MdC, and DwC. Of these, UpC was the most effective competitor for the formation of the DNA–protein complexes, and MdC inhibited

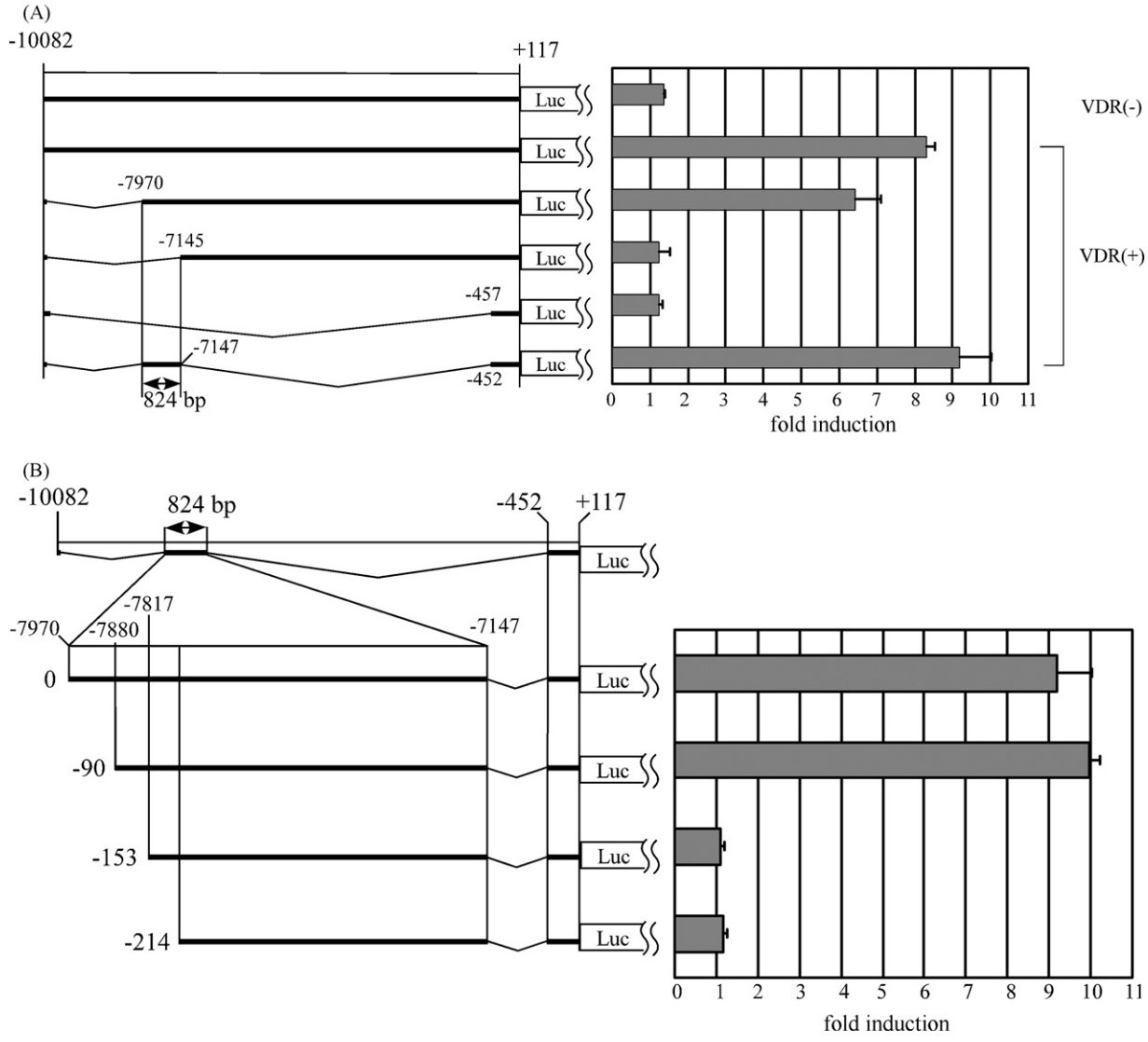

Fig. 1 – Transcriptional activity of several deletion mutants of human *MDR1* in the 5′-upstream region induced by 1,25-$(OH)_2D_3$. The 5′-upstream region of the *MDR1* gene was cloned into pGL4.12, as indicated on the left. Numbers are in reference to the transcriptional start site at +1. Luciferase activity was analyzed as described in Section 2. Fold induction was calculated as the ratio of luciferase activity in 1,25-$(OH)_2D_3$-treated cells to that of DMSO-treated cells, and is indicated on the right side of each column. Each value represents the mean ± S.D. of four independent experiments. (A) Schematic representations of pMD10082L, pMD7970L, pMD7145L, pMD457L and pMD*824L are shown from the top of the left side. (B) Schematic representations of pMD*824L, pMD*824Δ90L, pMD*824Δ153L, and pMD*824Δ214L are shown from the top of the left side.

complex formation to an extent similar to that of DwC (Fig. 2B). Similar competition assay results were obtained using MdC and DwC probes (Fig. 2C and D).

To identify the VDR/RXRα-binding site in these segments, shorter oligonucleotides containing two or three half-sites were used as competitors (Fig. 2B). The most efficient competitor for VDR/RXRα binding to UpC was DR4(I), followed by DR3, MdC3, DR4(III), and DR4(II). MdC5 lacking Hs6 of MdC was not able to compete for the UpC probe, indicating that Hs6 is necessary for MdC–VDR/RXRα binding.

Next, oligonucleotides including a set of 2 bp mutations in each of the half-sites (UpM1∼DwM12 in Fig. 2A) were used as competitors for EMSA. As shown in Fig. 2B, UpM1 including the Hs1 mutation in UpC competed for the UpC probe at the same level as the wild-type competitor. UpM3 including the Hs3 mutation in UpC competed slightly less efficiently than the wild-type. UpM2 including the Hs2 mutation in UpC failed to compete for UpC, indicating that Hs2 is essential for UpC–VDR/RXRα complex formation (Fig. 2B).

The result obtained using the MdC probe is shown in Fig. 2C. To determine which half-site of MdC3 is required for MdC–VDR/RXRα complex formation, the mutant oligonucleotides including the 2 bp mutations in the half-sites of MdC3 were used as competitors (MdM31, M33, and M4). MdM31 including the Hs4 mutation partially competed for MdC, but MdM33 containing the Hs5 mutation competed for MdC as effectively as the wild-type competitor. MdM4 including the Hs6 mutation in MdC3 failed to compete for

the MdC probe, indicating that Hs6 is essential for MdC3–VDR/RXRα complex formation. This result is consistent with the fact that MdC5, which lacks Hs6 of MdC, is not able to bind VDR/RXRα.

The result obtained using the DwC probe is shown in Fig. 2D. The Hs6 and Hs7 mutations in DwC (DwM4 and DwM7, respectively) did not affect the competition for DwC, whereas the Hs8 mutation caused reduced competition by DwM12 for

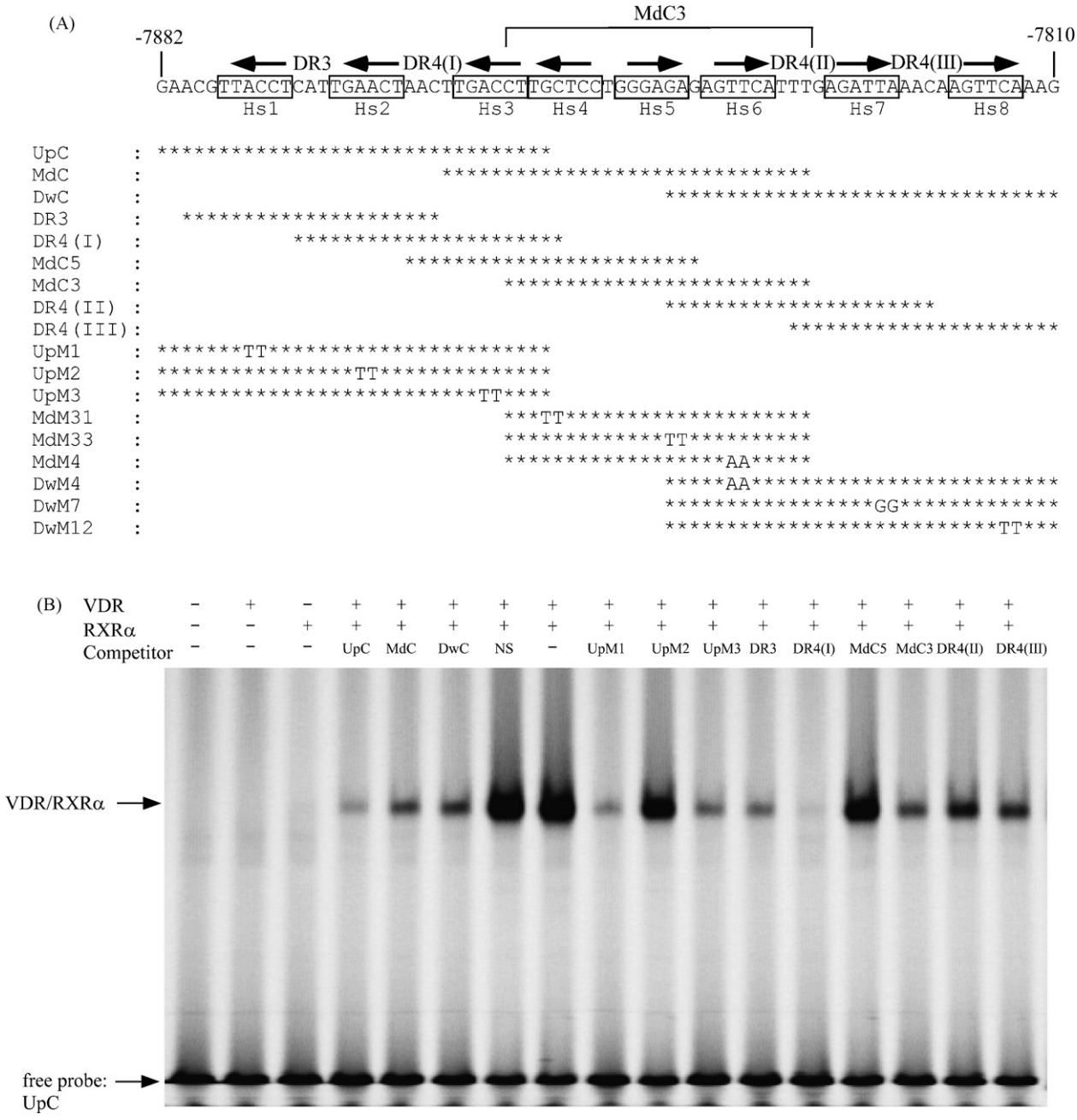

Fig. 2 – VDR binds to the putative VDREs in the region essential for VDR-mediated induction as a heterodimer with RXRα. (A) Oligonucleotide sequences used for EMSA. Putative half-sites (Hs1–8) predicted using JASPAR FAM are boxed, and arrows indicate the direction of the half-site. Numbers are in reference to the transcriptional start site at +1. Only nucleotides that differ from the wild-type are shown as letters; asterisks represent unchanged nucleotides. (B) EMSA was performed using a FITC-labeled UpC probe. The UpC probe was incubated in the absence or presence of in vitro translated VDR, RXRα, or both proteins, as described in Section 2. In parallel experiments, a competition assay was performed in the presence of a 50-fold molar excess of unlabeled oligonucleotide. "NS" indicates nonspecific competitor. The complexes were resolved by electrophoresis on a 6% Long Ranger gel. (C) EMSA was performed using a FITC-labeled MdC probe. The procedure was the same as that described in (B), except that a 15-fold molar excess of unlabeled oligonucleotides were used for the competition assay. "NS" indicates nonspecific competitor. (D) EMSA was performed using a FITC-labeled DwC probe. The procedure was the same as that described in (C). "NS" indicates nonspecific competitor.

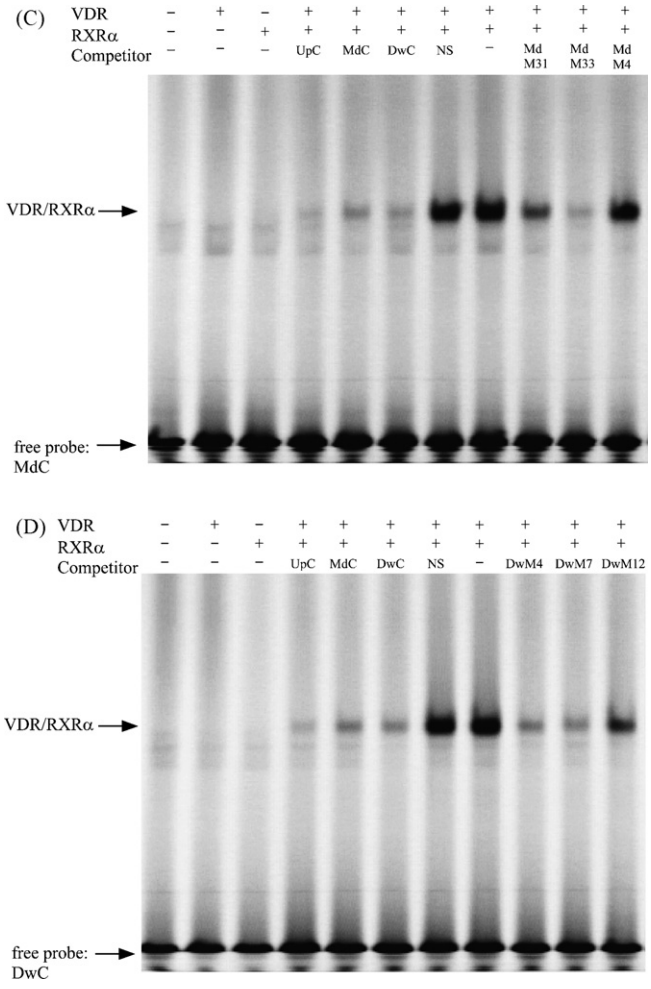

Fig. 2. (Continued).

the DwC probe. These results indicate that Hs8 is important for DwC–VDR/RXRα complex formation.

Taken together, VDR/RXRα is able to bind to several putative VDREs [DR4(I) and DR3 in UpC, MdC3 in MdC, and DR4(III) and DR4(II) in DwC] with different affinity. Additionally, Hs2, Hs6, and Hs8 are the most important half-sites in each segment for DNA–VDR/RXRα complex formation.

3.3. *Three molecules of VDR/RXRα are able to bind to the VDR-binding region at the same time*

Although we identified several sites competent to bind VDR/RXRα, the sites in this region are spaced relatively close to each other. The proximity of these VDR-binding sites might prevent the binding of VDR/RXRα to these sites. Therefore, the question that arises is how many molecules of VDR/RXRα bind to the VDR-binding region at the same time. To examine this, we performed EMSA using a longer probe (7882 probe in Fig. 3A) containing all the half-sites of the VDR-binding elements using different amounts of VDR/RXRα. At the highest concentration of the protein in the presence of 1,25-$(OH)_2D_3$, three shifted bands (upper, middle, and lower) were observed, although the intensity of the upper mobility band (3× VDR/RXRα in Fig. 3B) was weak. In the absence of 1,25-$(OH)_2D_3$, the upper band was very weak. The mobility of the lower band (1× VDR/RXRα in Fig. 3B) is the same as that of bands formed by UpC and DR4(II) probes (data not shown), to which one molecule of VDR/RXRα binds. This indicates that the lower band is the complex formed by the probe binding to one molecule of VDR/RXRα. As the amount of the protein was decreased, the intensity of the middle band (2× VDR/RXRα in Fig. 3B) decreased, while the intensity of the lower band remained constant. These results suggest that the middle band is the complex formed by the probe and two molecules of VDR/RXRα, and that three molecules of VDR/RXRα bind to this region with different affinities.

Furthermore, we performed EMSA in the presence of 1,25-$(OH)_2D_3$, which was required for the observation of three shifted bands (Fig. 3B), using longer probes containing at least one mutated half-site (Hs2, Hs6, and/or Hs8). These sites were shown to play an important role in DNA–VDR/RXRα complex formation in each segment, as shown in Fig. 2. The probes used for the EMSA are summarized in Fig. 3A. As shown in Fig. 3C, the upper bands in Fig. 3B disappeared when the M2, M4, and M12 probes were used; these probes each have one mutated half-site. In contrast, the M22, M23, and M30 probes, in which two of the three half-sites were mutated, caused the middle bands to disappear in addition to the upper bands.

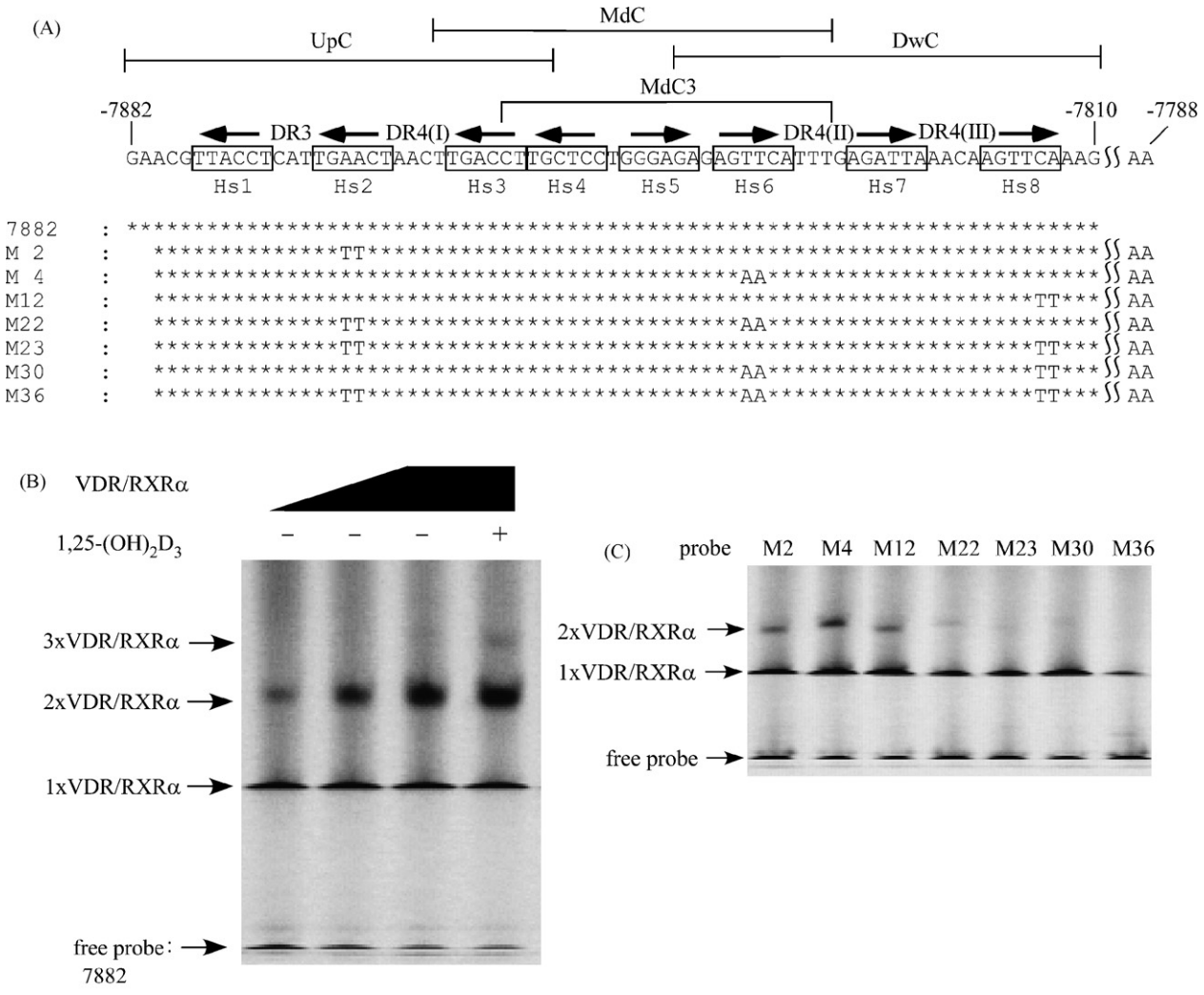

Fig. 3 – VDR/RXRα can bind to three VDR-binding sites at the same time. (A) The oligonucleotide sequences used for EMSA. Putative half-sites are boxed and arrows indicate the direction of the half-site. Numbers are in reference to the transcriptional start site at +1. Only nucleotides that differ from the wild-type are shown as letters; asterisks represent unchanged nucleotides. (B) EMSA was performed using a FITC-labeled 7882 probe. The probe was incubated with the increasing amount of in vitro translated VDR and RXRα as described in Section 2. The complexes were resolved by electrophoresis on a 2.8% Long Ranger gel. (C) EMSA was performed using several FITC-labeled probes, shown in (A). The probes were incubated with 1,25-$(OH)_2D_3$ and in vitro translated VDR and RXRα as described in Section 2. The complexes were resolved by electrophoresis on a 2.8% Long Ranger gel.

When all three half-sites were mutated (M36), the upper and middle bands disappeared and the lower band significantly decreased. These data indicate that one molecule of VDR/RXRα binds to each element including Hs2, Hs6, or Hs8. Consequently, three molecules of VDR/RXRα bind simultaneously to this region.

3.4. *VDR-binding sites located between −7880 and −7810 bp mediate the transactivation of MDR1 by 1,25-$(OH)_2D_3$*

In the experiments described above, we identified several VDR-binding sites. To test if these sites are functional, the same mutations introduced into the probes and competitors in the EMSA were introduced into the pMD*824Δ90L construct for use in the luciferase assay. The names of these mutants correspond to those used in the EMSA. The mutated regions of the constructs used for the luciferase assays are summarized in Fig. 4A. As shown in Fig. 4B, the mutation in Hs4 (M31) or Hs5 (M33), although slightly increased induction, had no apparent effect on inducibility, indicating that these half-sites play no significant role in induction by 1,25-$(OH)_2D_3$. The other mutations introduced into individual half-sites (M1, M2, M3, M4, M7, and M12) lead to decreased inducibility. The mutations introduced simultaneously into the two half-sites in two of the three segments resulted in a further decrease in induction by 1,25-$(OH)_2D_3$ (M28, M26, M29, M22, M27, M23, M30 in Fig. 4B). M22 and M29 (mutations in Hs2 and Hs6, and Hs3

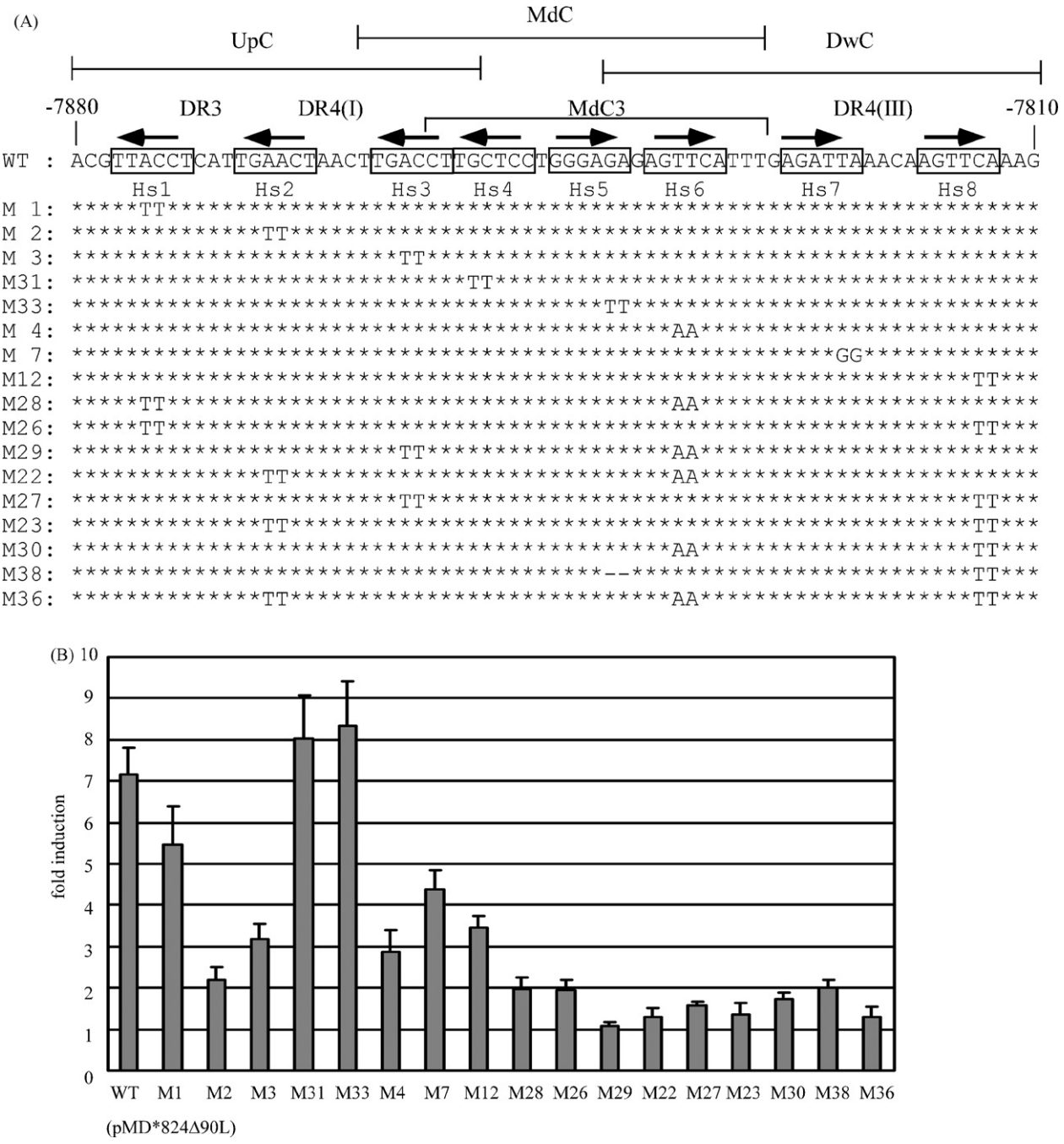

Fig. 4 – VDR-binding sites between −7880 and −7810 bp mediate the transcriptional activity of *MDR1* by 1,25-$(OH)_2D_3$. (A) Several mutations were introduced into the pMD*824Δ90L plasmid (designated WT). Putative half-sites are boxed and arrows indicate the direction of the half-site. Asterisks denote bases identical to the wild-type sequence and letters indicate the bases altered in the mutated sequences. The underbar indicates deletion of a nucleotide. Numbers are in reference to the transcriptional start site at +1. (B) The luciferase activity was analyzed as described in Section 2. The fold induction was calculated as the radio of luciferase activity in 1,25-$(OH)_2D_3$-treated cells to that of DMSO-treated cells. Each value represents the mean ± S.D. of four independent experiments.

and Hs6, respectively) almost abolished inducibility. The inducibility of M38, which has the deletion of one of the three repeated AGs located between Hs5 and Hs6 in M12 (Fig. 4A), decreased more than that of M12 (Fig. 4B). The inducibility of M36, which has mutations in all three segments, was also almost abolished. These results indicate that every half-site in the VDR-binding sites, except Hs4 and 5, is a functional VDRE and makes its own contribution to induction by 1,25-$(OH)_2D_3$. Furthermore, each VDRE additively contributes to the 1,25-$(OH)_2D_3$ response.

4. Discussion

Several studies have shown that 1,25-$(OH)_2D_3$ induces the expression of *MDR1* [7,22]. However, it remains unclear how 1,25-$(OH)_2D_3$ regulates *MDR1* expression. In this study, we demonstrated that the induction of *MDR1* by 1,25-$(OH)_2D_3$ is mediated by VDR/RXRα binding to the region located between −7.9 and −7.8 kbp upstream from the transcriptional start site of the human *MDR1* gene (Fig. 5).

As shown in Fig. 1B, the region located between −7880 and −7817 bp is essential for VDR-mediated induction. This result is the same as that obtained for TR-mediated induction [19]. Furthermore, this region overlaps with the previously identified PXR-, CAR-responsive region [3,4]. The eight putative half-sites (Hs1–Hs8) of VDREs were found in the region located between −7880 and −7810 bp (Fig. 2A). DR3, DR4(I), DR4(II), and DR4(III), which were previously designated by Geick et al., are composed of Hs1 and Hs2, Hs2 and Hs3, Hs6 and Hs7, and Hs7 and Hs8, respectively. Geick et al. reported that PXR/RXRα bound to these three DR4, with the highest affinity to DR4(III), and DR4(I) is an important element for PXR-mediated induction [3]. Burk et al. reported that CAR bound to DR4(I) and DR4(III) as a heterodimer with RXRα, and to the 5′-half-site of DR4(II) (designated as Hs6 in this study) as a monomer [4]. As for transcriptional activity, DR4(I) and the 5′-half-site of DR4(II) were reported to be important elements for CAR-mediated induction. Recently, we reported that TR/RXRα bound to UpC [including DR3 and DR4(I)] and DwC [including DR4(II) and DR4(III)] segments [19], whereas TR/RXRα did not bind to MdC located between UpC and DwC (M. Saeki, K. Kurose, unpublished data). Furthermore, two molecules of TR/RXRα bind simultaneously to the region, and several DRs contribute to the binding affinity in the order: DR4(I) > DR4(II) > DR3 ≈ DR4(III). As for the transcriptional activity, every direct repeat contributes to TR-mediated induction [19]. In the present study, we showed that VDR/RXRα bound to UpC (including Hs1–3), MdC (including Hs3–6), and DwC (including Hs6–8) (Fig. 2B). To date, no nuclear receptors other than VDR has been reported to bind to MdC by forming heterodimers with RXRα. Although Hs6, which is located at the overlapping region between MdC and DwC, significantly contributes to induction by CAR [4], the binding of CAR/RXRα to MdC and contribution of MdC to induction by CAR remains to be elucidated. As shown in Fig. 2B, the relative binding affinity of the VDR-binding elements is DR4(I) > DR3 > MdC3 > DR4(III) > DR4(II). Consequently, the relative binding ability of VDR to these elements located in this region is clearly different from that of PXR, CAR, and TR, though the VDR-responsive region overlaps with the PXR-, CAR-, and TR-responsive regions [3,4,19]. The overlapping of nuclear receptor-responsive regions was also observed on the other genes such as *CYP3A4* [23], in which PXR/RXRα and CAR/RXRα exhibited similar binding affinity toward proximal ER6 element [24]. On the nuclear receptor-responsive region of *MDR1* gene, PXR/RXRα and CAR/RXRα bound to DR4(I) with similar affinity, although PXR/RXRα bound to DR4(III) with the higher affinity than CAR/RXRα [4]. Although, relative binding affinities among TR/RXRα, VDR/RXRα, PXR/RXRα, and CAR/RXRα to these binding elements have not been examined, it is conceivable that cooperative effects of the nuclear receptors with different binding affinities, tissue distributions and ligand concentrations affect the expression of *MDR1*.

Three shifted bands were observed when a longer probe including all the half-sites of the VDR-binding elements was used for EMSA (Fig. 3A). The upper band (3× VDR/RXRα) was found to be enhanced by 1,25-$(OH)_2D_3$. This has also been observed in VDREs located in several genes such as human CYP24 [25-27] and is due to the stabilization of DNA–VDR/RXRα formation by 1,25-$(OH)_2D_3$ [26,28,29]. The relative binding affinity of the VDR-binding elements estimated from Fig. 2B is DR4(I) > DR3 > MdC3 > DR4(III) > DR4(II). The affinity was examined further by using each discrete oligonucleotide as a competitor and a probe. Fig. 3 indicates that three molecules of VDR/RXRα bind simultaneously to the region, and one molecule of VDR/RXRα binds to each element including Hs2, Hs6, or Hs8. It is obvious that the element including Hs8 is DR4(III); consequently, the element including Hs6 is in MdC3, but it could not be specified further. Although both DR3 and

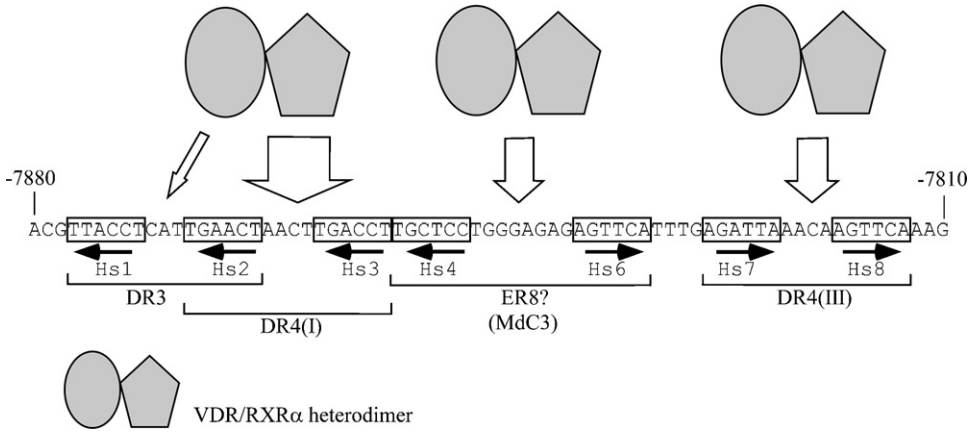

Fig. 5 – Three molecules of VDR/RXRα bind to VDREs located −7.9 to −7.8 kb upstream of the *MDR1* gene with different affinities. The nucleotide positions are shown relative to the transcription start site of *MDR1*. The half-sites of the VDREs are boxed with arrows. VDR/RXRα binds to DR3 or DR4(I), ER8, and/or DR4(III) with different affinity, which is denoted by the thickness of the arrow.

DR4(I) include Hs2 and each alone shows high affinity to VDR/RXRα, two molecules of VDR/RXRα are not able to simultaneously bind to DR4(I) and DR3 because they overlap with Hs2 (Fig. 2A). Therefore, judging from the binding affinity and decreased inducibility from the reporter gene assay (Fig. 4B), three molecules of VDR/RXRα would mainly bind to DR4(I), MdC3, and DR4(III) simultaneously. The middle band intensity of the M4 probe (MdC3 mutation) was stronger than that of the M2 and M12 probes (DR4(I) and DR4(III) mutations, respectively) (Fig. 3C). The difference in the middle band intensity between the M4 and M12 probes in Fig. 3C suggests that the two molecules of VDR/RXRα simultaneously bind to DR4(I) and DR4(III) more strongly than to DR4(I) and MdC3, though the relative binding affinity of VDR/RXRα to MdC3 was higher than to DR4(III), as shown in Fig. 2B. The proximity of DR4(I) and MdC3 might slightly restrict the binding of the two molecules of VDR/RXRα to those sites simultaneously.

We confirmed whether the VDR-binding sites contribute to induction using constructs with mutations in several half-sites (Fig. 4). DR4(I) and DR4(III) contribute to induction by 1,25-$(OH)_2D_3$, and so are functional VDREs. MdC3 includes Hs4, Hs5, and Hs6. Although the mutation in Hs6 (M4) resulted in reduced inducibility, both the mutation in Hs4 (M31) and that in Hs5 (M33) had little effect on induction (Fig. 4B). Precisely which half-site is paired with Hs6 is unclear, but Hs6 contributes to induction by 1,25-$(OH)_2D_3$. However, when one AG deletion of the three repeated AGs, which are located just upstream of Hs6 (Fig. 4A), was introduced into M12, the inducibility of the resulting mutant construct M38 decreased more than that of M12 (Fig. 4B). This indicates that the deletion results in reduced inducibility, suggesting that the half-site paired with Hs6 is located upstream of Hs6, and that the change in the spacer length between Hs6 and its upstream partner leads to the reduced inducibility. Hs4 is located upstream of Hs6, and the mutation introduced in Hs4 reduced binding activity (Fig. 2C, Md3M31). Therefore, the partner of Hs6 might be Hs4, although the mutation of Hs4 alone did not reduced inducibility by 1,25-$(OH)_2D_3$ (Fig. 4B, M31). If Hs4 and Hs6 are partners, then they are an everted repeat by 8 nucleotides (ER8). The mutation in Hs1 (Fig. 4B, M1, M28, and M26), namely the mutation in DR3, caused somewhat decreased activity. Thus, DR3 can function as a VDRE, suggesting that DR3 serves as an auxiliary function of the neighboring DR4(I) element.

Double mutations in the different segments result in substantial reduction in induction by 1,25-$(OH)_2D_3$ (Fig. 4). Among them, the double mutations in DR4(I) and ER8 of MdC3 resulted in an almost complete loss of inducibility (M22 and M29 in Fig. 4B). In M22, only DR4(III) is a wild-type motif, and in M29, DR3 is a wild-type motif in addition to DR4(III). Therefore, DR4(III) alone or in combination with DR3 might be incapable of induction. However, DR4(III) works cooperatively in combination with DR4(I) and/or MdC3 (compare M2 with M23, M4 with M30, and WT with M12 in Fig. 4B). These results indicate that the additive binding of VDR/RXRα to several VDREs results in additional enhancement of *MDR1* induction by 1,25-$(OH)_2D_3$.

Previous reports showed that Caco-2 cells are clearly less sensitive to the inductive effect of 1,25-$(OH)_2D_3$ compared with LS180 cells [7,30]. The VDR mRNA level in Caco-2 cells is lower than that in LS180 cells (twofold higher band intensity in LS180 cells) [9]. Additionally, the ligand-binding assay showed that LS180 and Caco-2 have VDR levels of 118 and 63 fmol/mg protein, respectively [31]. In our preliminary luciferase reporter experiment using LS180 cells transfected by pMD*824Δ90L, which contains VDREs, we observed transcriptional induction by 1,25-$(OH)_2D_3$ even in the absence of VDR expression plasmid (data not shown). Thus, the difference in response to 1,25-$(OH)_2D_3$ between these cells may reflect the amount of VDR/RXRα, which binds to the VDREs in the *MDR1* gene. VDR is expressed abundantly in the human intestine (approximately 250 fmol/mg protein) [32,33]. Thus, it is possible that 1,25-$(OH)_2D_3$ is involved in intestinal *MDR1* expression under normal physical conditions. Recent reports demonstrated that CYP27B1, which has an important role in the synthesis of 1,25-$(OH)_2D_3$, is expressed in human intestine [34–36]. In addition, extrarenally produced 1,25-$(OH)_2D_3$ primarily serves as an autocrine/paracrine factor with cell-specific functions [37,38]. Therefore, 1,25-$(OH)_2D_3$ levels in the intestine might be relatively high, whereas serum 1,25-$(OH)_2D_3$ levels are usually controlled at approximately 100 pmol/L. *MDR1* expression levels are different between individuals [20], and these variations might affect the toxicity and efficacy of drugs. Intestinal vitamin D status, which might be affected by, for example, intestinal CYP27B1 and circulating 25-hydroxyvitamin D_3 levels, might partially contribute to differences between individuals in *MDR1* expression.

Recently, it has been shown that 1,25-$(OH)_2D_3$ is involved in the formation of tight junctions, which seal the paracellular space between adjacent cells to create a primary barrier, in intestinal epithelial cells [39]. Kutuzova et al. reported that 1,25-$(OH)_2D_3$ causes increases in the expression of several phase I and phase II enzymes such as CYP3As in rat intestine after injection of 1,25-$(OH)_2D_3$ into vitamin D-deficient rats [40]. These data indicate that 1,25-$(OH)_2D_3$ would play an important role in the intestinal epithelial barrier function against xenobiotics by regulating tight junctions and inducing several drug-metabolizing enzymes and *MDR1*.

The induction of P-gp by 1,25-$(OH)_2D_3$ could lead to an increase in the systemic efflux of co-administrated drugs that serve as P-gp substrates. For instance, Olaizola et al. reported that the uptake of [^{99m}Tc]-sestamibi by the parathyroid glands of uremic patients was suppressed by pulse administration of 1,25-$(OH)_2D_3$ [13]. [^{99m}Tc]-Sestamibi is a substrate of P-gp and is excreted by P-gp [11,12], suggesting that P-gp induction by 1,25-$(OH)_2D_3$ leads to increased efflux of [^{99m}Tc]-sestamibi [13]. Vitamin D derivatives are widely prescribed, therefore, consideration for drug–drug interaction mediated by induction of P-gp by vitamin D derivatives should probably be paid.

In summary, we have demonstrated that the induction of *MDR1* by 1,25-$(OH)_2D_3$ is mediated by VDR/RXRα binding to VDREs located between −7.9 and −7.8 kbp upstream of the human *MDR1* gene, and that three molecules of VDR/RXRα are able to simultaneously bind with different affinities. DR3, DR4(I), MdC3 (ER8) and DR4(III) are functional VDREs, and the contribution of each VDRE toward inducibility is different (Fig. 5). Furthermore, each VDRE additively contributes to the 1,25-$(OH)_2D_3$ response.

Acknowledgements

We thank Dr. Shuichi Koizumi (Yamanashi University) for providing the human RXRα cDNA. This work was supported in part by grants from the Ministry of Health, Labor and Welfare of Japan and the Japan Health Sciences Foundation (Research on Publicly Essential Drugs and Medical Devices).

REFERENCES

[1] Marchetti S, Mazzanti R, Beijnen JH, Schellens JH. Concise review: clinical relevance of drug drug and herb drug interactions mediated by the ABC transporter ABCB1 (MDR1, P-glycoprotein). Oncologist 2007;12:927–41.
[2] Wacher VJ, Wu CY, Benet LZ. Overlapping substrate specificities and tissue distribution of cytochrome P450 3A and P-glycoprotein: implications for drug delivery and activity in cancer chemotherapy. Mol Carcinog 1995;13: 129–34.
[3] Geick A, Eichelbaum M, Burk O. Nuclear receptor response elements mediate induction of intestinal MDR1 by rifampin. J Biol Chem 2001;276:14581–7.
[4] Burk O, Arnold KA, Geick A, Tegude H, Eichelbaum M. A role for constitutive androstane receptor in the regulation of human intestinal MDR1 expression. Biol Chem 2005;386:503–13.
[5] Bertilsson G, Heidrich J, Svensson K, Asman M, Jendeberg L, Sydow-Backman M, et al. Identification of a human nuclear receptor defines a new signaling pathway for CYP3A induction. Proc Natl Acad Sci USA 1998;95:12208–13.
[6] Moore LB, Parks DJ, Jones SA, Bledsoe RK, Consler TG, Stimmel JB, et al. Orphan nuclear receptors constitutive androstane receptor and pregnane X receptor share xenobiotic and steroid ligands. J Biol Chem 2000;275:15122–7.
[7] Aiba T, Susa M, Fukumori S, Hashimoto Y. The effects of culture conditions on CYP3A4 and MDR1 mRNA induction by 1alpha,25-dihydroxyvitamin D(3) in human intestinal cell lines, Caco-2 and LS180. Drug Metab Pharmacokinet 2005;20:268–74.
[8] Pfrunder A, Gutmann H, Beglinger C, Drewe J. Gene expression of CYP3A4, ABC-transporters (MDR1 and MRP1–MRP5) and hPXR in three different human colon carcinoma cell lines. J Pharm Pharmacol 2003;55:59–66.
[9] Thummel KE, Brimer C, Yasuda K, Thottassery J, Senn T, Lin Y, et al. Transcriptional control of intestinal cytochrome P-4503A by 1alpha,25-dihydroxy vitamin D3. Mol Pharmacol 2001;60:1399–406.
[10] Patel J, Pal D, Vangal V, Gandhi M, Mitra AL. Transport of HIV-protease inhibitors across 1 alpha,25di-hydroxy vitamin D3-treated Calu-3 cell monolayers: modulation of P-glycoprotein activity. Pharm Res 2002;19:1696–703.
[11] Piwnica-Worms D, Chiu ML, Budding M, Kronauge JF, Kramer RA, Croop JM. Functional imaging of multidrug-resistant P-glycoprotein with an organotechnetium complex. Cancer Res 1993;53:977–84.
[12] Yamaguchi S, Yachiku S, Hashimoto H, Kaneko S, Nishihara M, Niibori D, et al. Relation between technetium 99m-methoxyisobutylisonitrile accumulation and multidrug resistance protein in the parathyroid glands. World J Surg 2002;26:29–34.
[13] Olaizola I, Zingraff J, Heuguerot C, Fajardo L, Leger A, Lopez J, et al. [(99m)Tc]-sestamibi parathyroid scintigraphy in chronic haemodialysis patients: static and dynamic explorations. Nephrol Dial Transplant 2000;15:1201–6.
[14] Drocourt L, Ourlin JC, Pascussi JM, Maurel P, Vilarem MJ. Expression of CYP3A4, CYP2B6, and CYP2C9 is regulated by the vitamin D receptor pathway in primary human hepatocytes. J Biol Chem 2002;277:25125–32.
[15] Schrader M, Nayeri S, Kahlen JP, Muller KM, Carlberg C. Natural vitamin D3 response elements formed by inverted palindromes: polarity-directed ligand sensitivity of vitamin D3 receptor-retinoid X receptor heterodimer-mediated transactivation. Mol Cell Biol 1995;15:1154–61.
[16] Tavera-Mendoza L, Wang TT, Lallemant B, Zhang R, Nagai Y, Bourdeau V, et al. Convergence of vitamin D and retinoic acid signalling at a common hormone response element. EMBO Rep 2006;7:180–5.
[17] Matilainen M, Malinen M, Saavalainen K, Carlberg C. Regulation of multiple insulin-like growth factor binding protein genes by 1alpha,25-dihydroxyvitamin D3. Nucleic Acids Res 2005;33:5521–32.
[18] Seoane S, Perez-Fernandez R. The vitamin D receptor represses transcription of the pituitary transcription factor Pit-1 gene without involvement of the retinoid X receptor. Mol Endocrinol 2006;20:735–48.
[19] Kurose K, Saeki M, Tohkin M, Hasegawa R. Thyroid hormone receptor mediates human MDR1 gene expression—identification of the response region essential for gene expression. Arch Biochem Biophys 2008;474: 82–90.
[20] Nakamura T, Sakaeda T, Ohmoto N, Tamura T, Aoyama N, Shirakawa T, et al. Real-time quantitative polymerase chain reaction for MDR1, MRP1, MRP2, and CYP3A-mRNA levels in Caco-2 cell lines, human duodenal enterocytes, normal colorectal tissues, and colorectal adenocarcinomas. Drug Metab Dispos 2002;30:4–6.
[21] Kurose K, Ikeda S, Koyano S, Tohkin M, Hasegawa R, Sawada J. Identification of regulatory sites in the human PXR (NR1I2) promoter region. Mol Cell Biochem 2006;281:35–43.
[22] Hochman JH, Chiba M, Nishime J, Yamazaki M, Lin JH. Influence of P-glycoprotein on the transport and metabolism of indinavir in Caco-2 cells expressing cytochrome P-450 3A4. J Pharmacol Exp Ther 2000;292: 310–8.
[23] Pascussi JM, Gerbal-Chaloin S, Drocourt L, Maurel P, Vilarem MJ. The expression of CYP2B6, CYP2C9 and CYP3A4 genes: a tangle of networks of nuclear and steroid receptors. Biochim Biophys Acta 2003;1619:243–53.
[24] Xie W, Barwick JL, Simon CM, Pierce AM, Safe S, Blumberg B, et al. Reciprocal activation of xenobiotic response genes by nuclear receptors SXR/PXR and CAR. Genes Dev 2000;14:3014–23.
[25] Lempiainen H, Molnar F, Macias Gonzalez M, Perakyla M, Carlberg C. Antagonist- and inverse agonist-driven interactions of the vitamin D receptor and the constitutive androstane receptor with corepressor protein. Mol Endocrinol 2005;19:2258–72.
[26] Toell A, Polly P, Carlberg C. All natural DR3-type vitamin D response elements show a similar functionality in vitro. Biochem J 2000;352(Pt 2):301–9.
[27] Kim S, Yamazaki M, Zella LA, Shevde NK, Pike JW. Activation of receptor activator of NF-kappaB ligand gene expression by 1,25-dihydroxyvitamin D3 is mediated through multiple long-range enhancers. Mol Cell Biol 2006;26:6469–86.
[28] Quack M, Carlberg C. Ligand-triggered stabilization of vitamin D receptor/retinoid X receptor heterodimer conformations on DR4-type response elements. J Mol Biol 2000;296:743–56.
[29] Kimmel-Jehan C, Jehan F, DeLuca HF. Salt concentration determines 1,25-dihydroxyvitamin D3 dependency of vitamin D receptor–retinoid X receptor–vitamin D-

responsive element complex formation. Arch Biochem Biophys 1997;341:75–80.
[30] Engman HA, Lennernas H, Taipalensuu J, Otter C, Leidvik B, Artursson P. CYP3A4, CYP3A5, and MDR1 in human small and large intestinal cell lines suitable for drug transport studies. J Pharm Sci 2001;90:1736–51.
[31] Shabahang M, Buras RR, Davoodi F, Schumaker LM, Nauta RJ, Evans SR. 1,25-Dihydroxyvitamin D3 receptor as a marker of human colon carcinoma cell line differentiation and growth inhibition. Cancer Res 1993;53:3712–8.
[32] Ebeling PR, Sandgren ME, DiMagno EP, Lane AW, DeLuca HF, Riggs BL. Evidence of an age-related decrease in intestinal responsiveness to vitamin D: relationship between serum 1,25-dihydroxyvitamin D3 and intestinal vitamin D receptor concentrations in normal women. J Clin Endocrinol Metab 1992;75:176–82.
[33] Kinyamu HK, Gallagher JC, Prahl JM, DeLuca HF, Petranick KM, Lanspa SJ. Association between intestinal vitamin D receptor, calcium absorption, and serum 1,25 dihydroxyvitamin D in normal young and elderly women. J Bone Miner Res 1997;12:922–8.
[34] Bises G, Kallay E, Weiland T, Wrba F, Wenzl E, Bonner E, et al. 25-Hydroxyvitamin D3-1alpha-hydroxylase expression in normal and malignant human colon. J Histochem Cytochem 2004;52:985–9.
[35] Tangpricha V, Flanagan JN, Whitlatch LW, Tseng CC, Chen TC, Holt PR, et al. 25-Hydroxyvitamin D-1alpha-hydroxylase in normal and malignant colon tissue. Lancet 2001;357:1673–4.
[36] Walters JR, Balesaria S, Khair U, Sangha S, Banks L, Berry JL. The effects of Vitamin D metabolites on expression of genes for calcium transporters in human duodenum. J Steroid Biochem Mol Biol 2007;103:509–12.
[37] Dusso AS, Brown AJ, Slatopolsky E. Vitamin D. Am J Physiol Renal Physiol 2005;289:F8–28.
[38] Hewison M, Burke F, Evans KN, Lammas DA, Sansom DM, Liu P, et al. Extra-renal 25-hydroxyvitamin D3-1alpha-hydroxylase in human health and disease. J Steroid Biochem Mol Biol 2007;103:316–21.
[39] Kong J, Zhang Z, Musch MW, Ning G, Sun J, Hart J, et al. Novel role of the vitamin D receptor in maintaining the integrity of the intestinal mucosal barrier. Am J Physiol Gastrointest Liver Physiol 2008;294:G208–16.
[40] Kutuzova GD, DeLuca HF. 1,25-Dihydroxyvitamin D3 regulates genes responsible for detoxification in intestine. Toxicol Appl Pharmacol 2007;218:37–44.